Supplementary Information (SI) for Nanoscale.

Supplementary Material

Effect of Functional Group Modification on the Adsorption Performance of Cerium-Based MOFs

YunFeng Li[a,b], YaXi Zhang[a,b] , Jin Liang[a,b,*], Li Zhang [a,b], Na Liu[a], Lu Li[a], ZiQuan Zeng[a,b]

[a]*School of Materials and Energy, Central South University of Forestry and Technology, Changsha, 410004, P. R. China*

[b]*Hunan Province Key Laboratory of Materials Surface & Interface Science and Technology, Changsha, P. R. China*

∗Corresponding author.

E-mail: ljcfstu@163.com.

Text S1 MB standard curve

A 100 mg/L MB stock solution was prepared. Thereafter, 0, 1, 2, 3, 4, and 5 mL of the stock solution were transferred to six 100 mL volumetric flasks and then diluted with deionized water-yielding MB standard solutions at concentrations of 0, 1, 2, 3, 4, and 5 mg/L, respectively. The absorbance of each MB standard solution was measured at 664 nm with a UV-Vis spectrophotometer. A calibration curve was plotted with absorbance (y) against MB concentration (x). As shown in Fig. S1, the linear relationship between MB concentration and absorbance yielded the regression equation $y = 0.15209x + 0.01295$ ($R^2 = 0.99$).

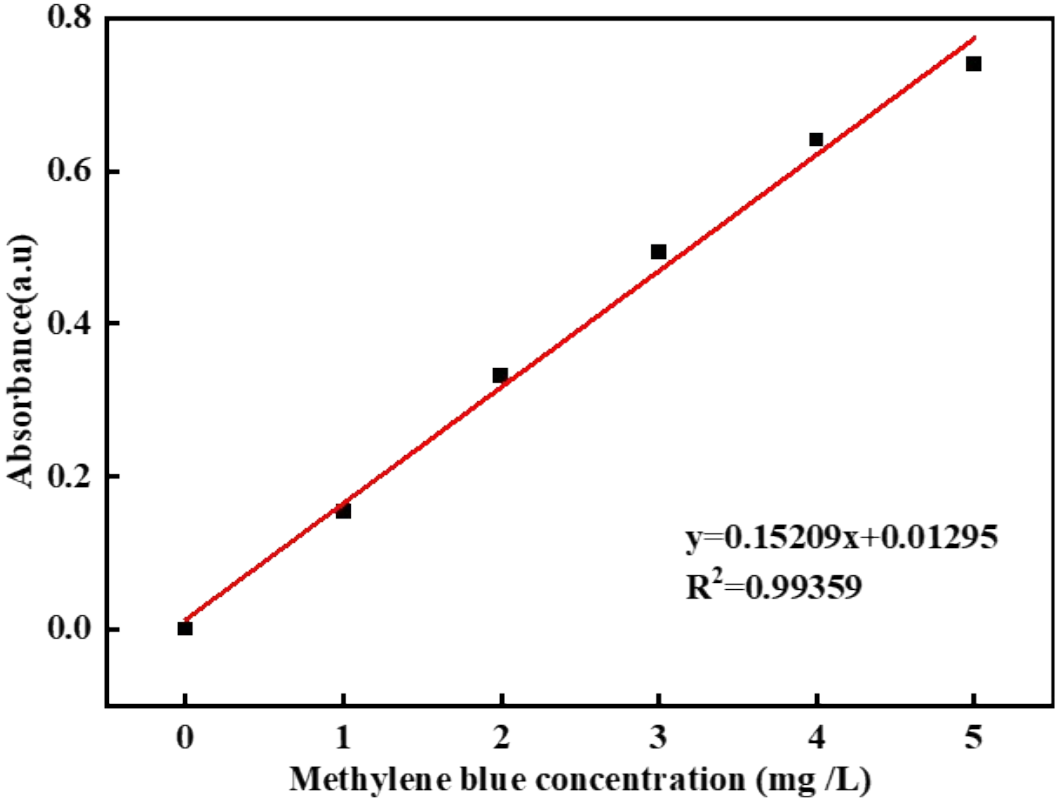

Fig. S1 Standard curve of Methylene Blue concentration.

Text S2 Cu(II) standard curve

The concentration of Cu(II) was determined following GB 7474-87 (National Standard of the People's Republic of China for Water Quality—Determination of Copper). The detection principle is as follows: under alkaline conditions, Cu(II) reacts with sodium diethyldithiocarbamate trihydrate (hereafter abbreviated as "copper reagent"), forming a yellowish-brown complex with a maximum absorption

wavelength of 452 nm. Five grams of copper reagent was weighed, dissolved in deionized water, diluted to 250 mL in a 250 mL volumetric flask, and the resulting solution was stored in a brown glass bottle. A 100 mg/L Cu(II) standard solution was prepared. Subsequently, 0, 2, 4, 6, 8, and 10 mL of the prepared Cu(II) standard solution were transferred to six 100 mL volumetric flasks, respectively. Next, 10 mL of the prepared copper reagent solution was added to each flask, the pH was adjusted to 9 with ammonia solution, and each solution was diluted to volume with deionized water—yielding Cu(II) standard solutions with final concentrations of 0, 2, 4, 6, 8, and 10 mg/L, respectively. The absorbance of each Cu(II) standard solution was measured at 452 nm. A calibration curve was plotted with absorbance values on the y-axis (vertical axis) and Cu(II) concentrations on the x-axis (horizontal axis). The linear relationship between Cu(II) concentration and absorbance yielded the regression equation y = 0.11759x + 0.0319 (R^2 = 0.99), as shown in Fig. S2.

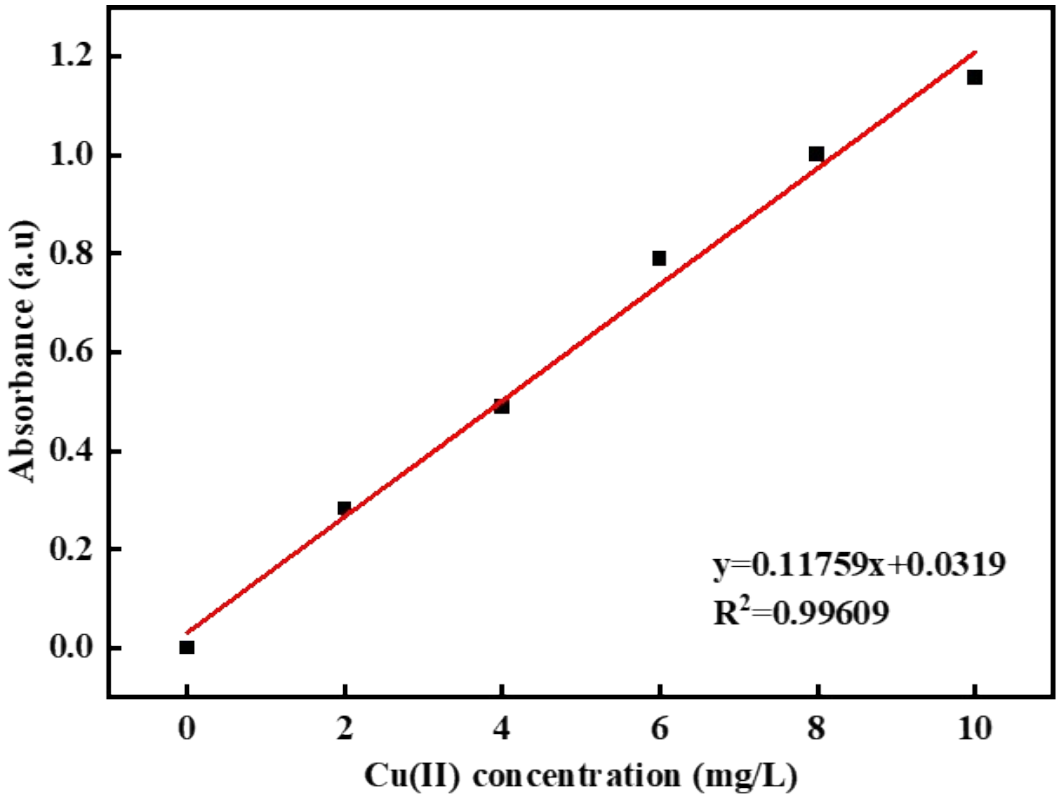

Fig. S2 Standard curve of Cu(II) concentration.

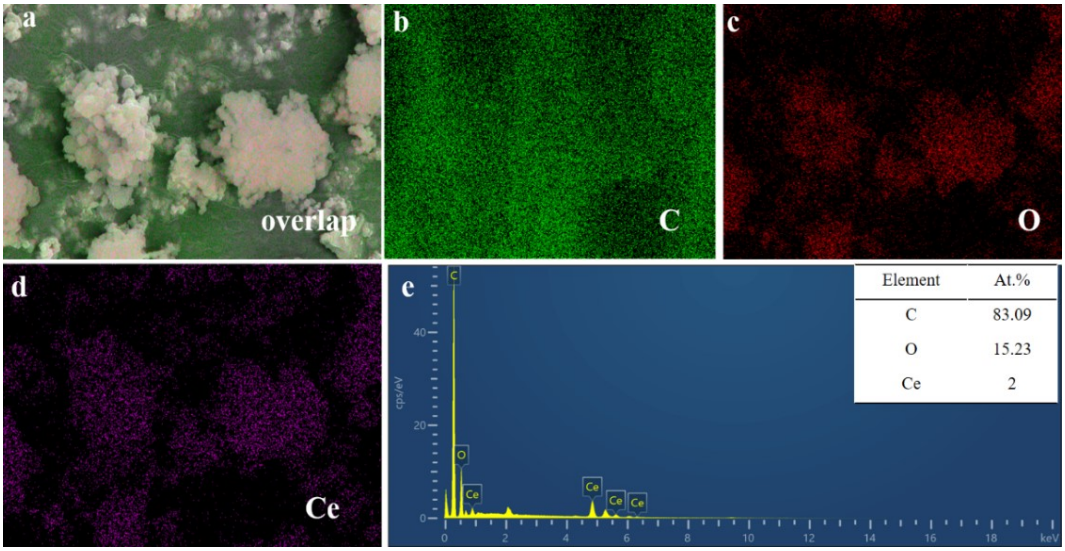

Fig. S3 EDX data and images of UiO-66(Ce).

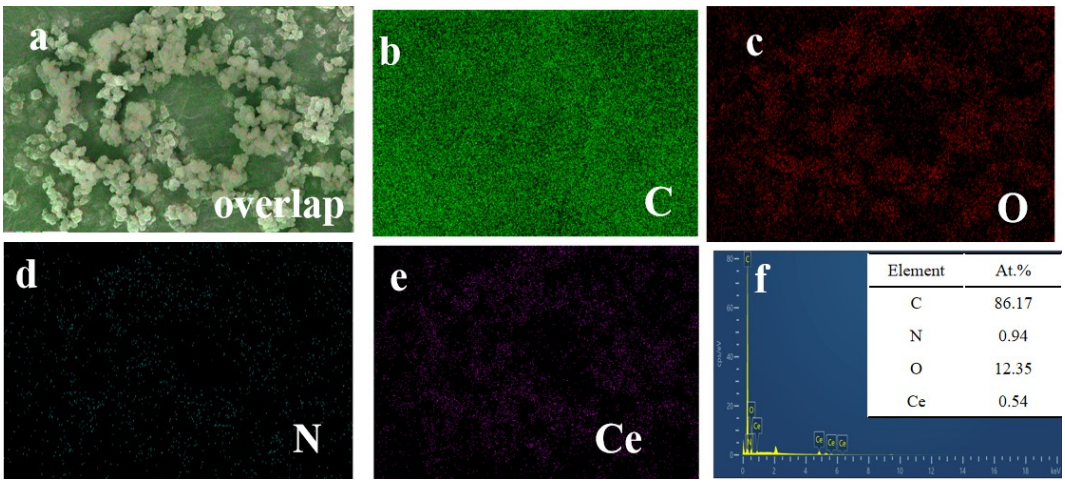

Fig. S4 EDX data and images of (a-e) UiO-66(Ce)-NO_2 (f) UiO-66(Ce)-NO_2.

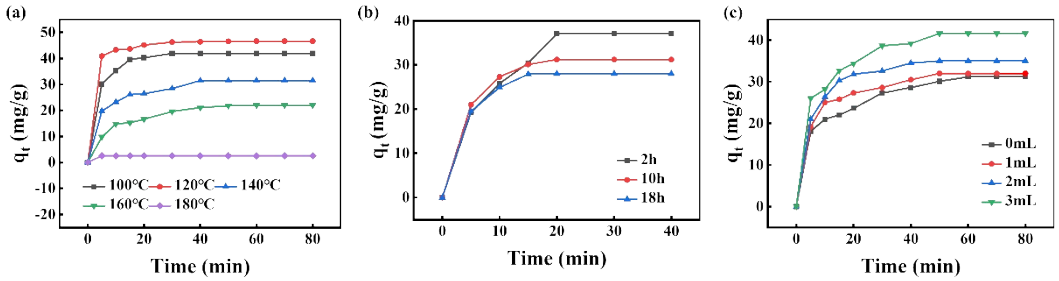

Fig. S5 (a) Adsorption curves of UiO-66(Ce) for MB at different hydrothermal temperatures; (b) Adsorption curves of UiO-66(Ce) for MB at different hydrothermal durations; (c) Adsorption curves of UiO-66(Ce) for MB at different acetic acid dosages.

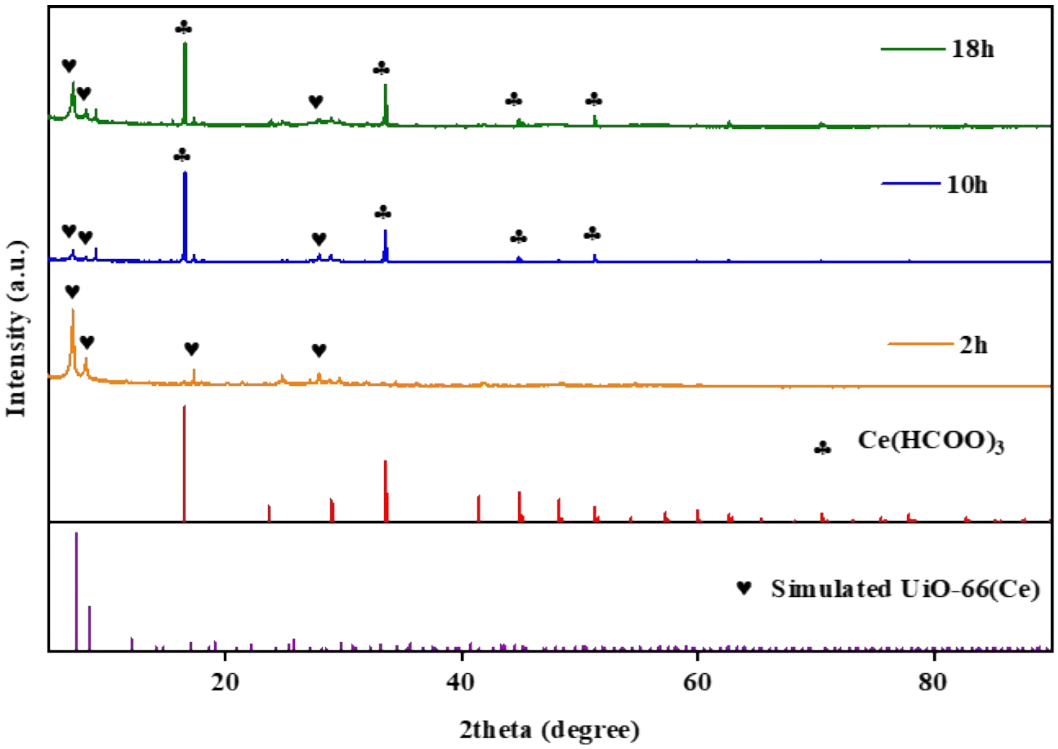

Fig. S6 XRD patterns of UiO-66(Ce) synthesized under different hydrothermal conditions.

Table S1 Saturation adsorption data of MB by UiO-66 series and selected MOFs.

Absorbents	q_m (mg/g)	Ref
MIL-121	27.8	1
UiO-66-NO_2	41.7	2
UiO-66-$(COOH)_2$	80.66	3
UiO-66-0.25$(COOH)_2$	87	4
UiO-66-0.5$(COOH)_2$	90	4
UiO-66	90.88	5
UiO-66-0.75$(COOH)_2$	94	4
UiO-66-NH_2	96.45	5
UiO-66-$(OH)_2$/GO	100	6
UiO-66(Ce)-NO_2	191	this study

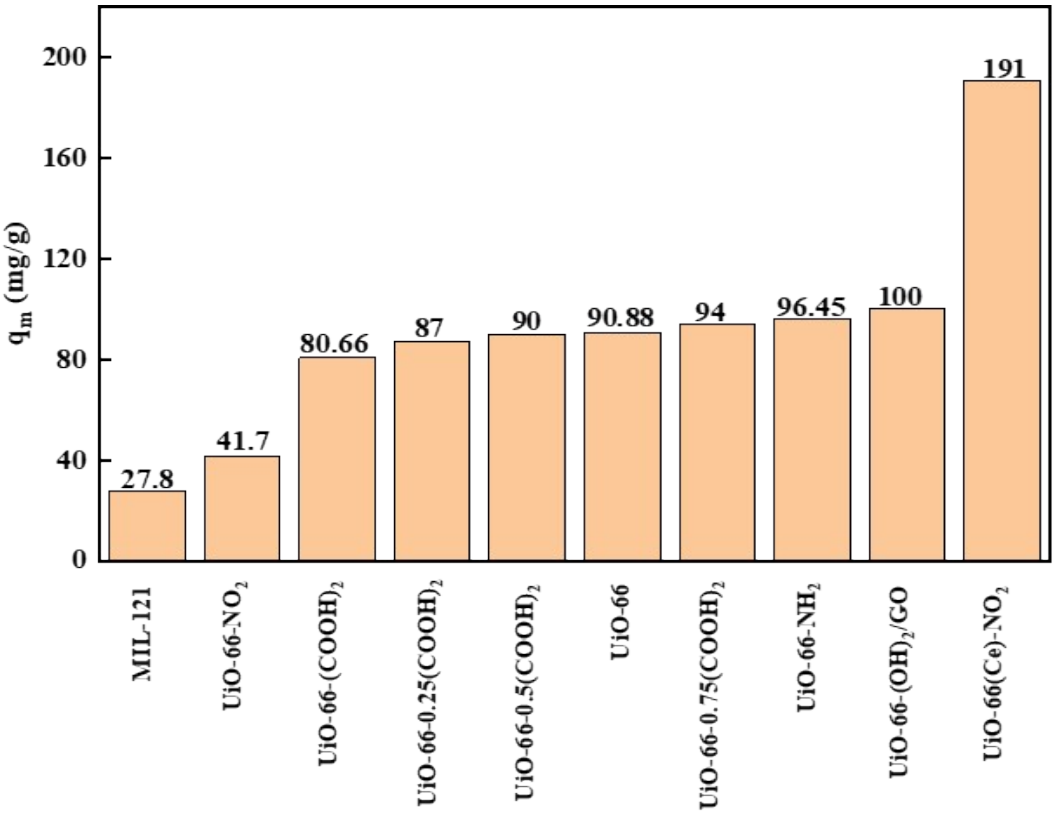

Fig. S7 Detailed comparison of methyl bromide adsorption capacities between the UiO-66 series and selected MOFs.

Table S2 Saturated adsorption capacity of Cu(II) on different materials.

Adsorption	q_m (mg/g)	Ref
FOCC	13.55	7
Activated carbon	43.47	8
SBA-15-DETA	57.50	9
PNIPAM-Co-AA	67.25	10
PGCB	100.00	11
ZIF-8	116.98	12
Cu-ZIF-8	135.12	13
MSH@SH NPs	190.00	14
Zn-mI-BDC	200.00	15
UiO-66(Ce)-NO_2	208.68	this study

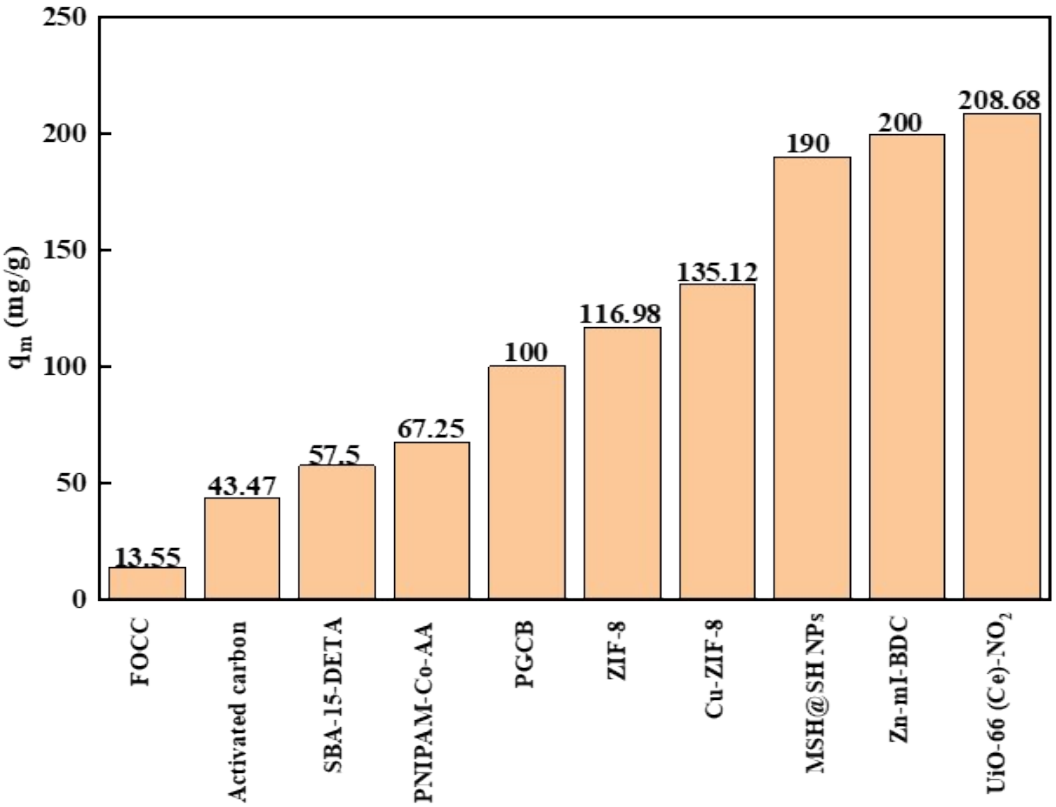

Fig. S8 Saturated adsorption capacity of Cu(II) on different materials.

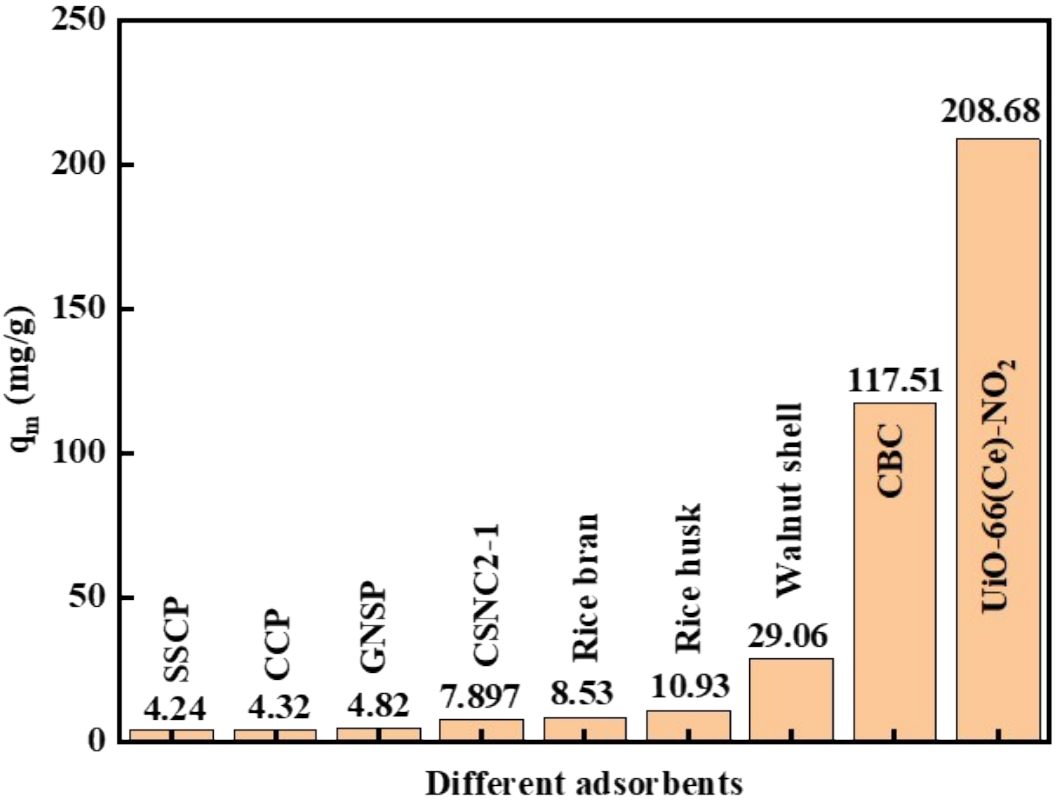

Fig S9 Saturated adsorption capacity of natural materials for Cu(II).

References

1. Hu, N.; Hang, F.; Li, K., et al., Temperature-regulated formation of hierarchical pores and defective sites in MIL-121 for enhanced adsorption of cationic and anionic dyes. *Sep. Purif. Technol.* **2023,** *314*, 123650.

2. Dinh, H. T.; Tran, N. T.; Trinh, D. X. J. J. o. A. M. i. C., Investigation into the Adsorption of Methylene Blue and Methyl Orange by UiO-66-NO_2 Nanoparticles. *Journal of Analytical Methods in Chemistry* **2021,** *2021* (1), 5512174.

3. Lei, Y. T.; Zhao, J. L.; Song, H. M., et al., Enhanced adsorption of dyes by functionalized UiO-66 nanoparticles: Adsorption properties and mechanisms. *J. Mol. Struct.* **2023,** *1292*, 136111.

4. Li, T. T.; Liu, Y. M.; Wang, T., et al., Regulation of the surface area and surface charge property of MOFs by multivariate strategy: Synthesis, characterization, selective dye adsorption and separation. *Microporous Mesoporous Mater.* **2018,** *272*, 101-108.

5. Chen, Q.; He, Q.; Lv, M., et al., Selective adsorption of cationic dyes by UiO-66-NH_2. *Appl. Surf. Sci.* **2015,** *327*, 77-85.

6. Sun, Y.; Chen, M.; Liu, H., et al., Adsorptive removal of dye and antibiotic from water with functionalized zirconium-based metal organic framework and graphene oxide composite nanomaterial Uio-66-$(OH)_2$/GO. *Appl. Surf. Sci.* **2020,** *525*, 146614.

7. Yuan, X. L.; Chen, X. X.; Zhou, Y. F., et al., Effective Removal of Copper(II) Ion from Polluted Water Using Ferric Oxide-Chitosan Composite: Kinetic, Equilibrium and Adsorption Mechanism Studies. *Water Air Soil Pollut.* **2025,** *236* (1), 27.

8. Demiral, H.; Güngör, C. J. J. o. c. p., Adsorption of copper (II) from aqueous solutions on activated carbon prepared from grape bagasse. *Journal of cleaner production* **2016,** *124*, 103-113.

9. Yang, Y.; Cao, X.; Ma, Z. P., et al., Adsorption of Cu(II) and Cr(III) ions on SBA-15 mesoporous silica functionalized by branched amine. *Desalination and Water Treatment* **2021,** *213*, 358-370.

10. Chen, J.; Ahmad, A.; Ooi, B. J. J. o. E. C. E., Poly (N-isopropylacrylamide-co-acrylic acid) hydrogels for copper ion adsorption: Equilibrium isotherms, kinetic and

thermodynamic studies. *Journal of Environmental Chemical Engineering* **2013,** *1* (3), 339-348.

11. Igberase, E.; Osifo, P.; Ofomaja, A. J. J. o. e. c. e., The adsorption of copper (II) ions by polyaniline graft chitosan beads from aqueous solution: equilibrium, kinetic and desorption studies. *Journal of environmental chemical engineering* **2014,** *2* (1), 362-369.

12. Zhou Long, Z. L.; Li Na, L. N.; Owens, G., et al., Simultaneous removal of mixed contaminants, copper and norfloxacin, from aqueous solution by ZIF-8. *Chem. Eng. J.* **2019**, 628-637.

13. Sun, S. W.; Yang, Z. H.; Cao, J., et al., Copper-doped ZIF-8 with high adsorption performance for removal of tetracycline from aqueous solution. *J. Solid State Chem.* **2020,** *285*, 121219.

14. Mane, S. M.; Raorane, C. J.; Shin, J. C. J. N., Synthesis of mesoporous silica adsorbent modified with mercapto–amine groups for selective adsorption of Cu^{2+} Ion from aqueous solution. *Nanomaterials* **2022,** *12* (18), 3232.

15. Latrach, Z.; Moumen, E.; Kounbach, S., et al., Mixed-ligand strategy for the creation of hierarchical porous ZIF-8 for enhanced adsorption of copper ions. *ACS omega* **2022,** *7* (18), 15862-15869.